

Study of Electron–Phonon Coupling Dynamics in Au Nanorods by Transient Depolarization Measurements

Ying Jiang,[†] Hai-Yu Wang,^{*,†} Li-Ping Xie,[†] Bing-Rong Gao,[†] Lei Wang,^{†,‡} Xu-Lin Zhang,[†] Qi-Dai Chen,[†] Han Yang,[†] Hong-Wei Song,[†] and Hong-Bo Sun^{*,†,‡}

State Key Laboratory on Integrated Optoelectronics, College of Electronic Science and Engineering, Jilin University, 2699 Qianjin Street, Changchun 130012, China, and College of Physics, Jilin University, 119 Jiefang Road, Changchun 130023, China

Received: November 16, 2009; Revised Manuscript Received: December 22, 2009

Electron–phonon (e-ph) coupling dynamics in Au nanorods are studied with femtosecond transient depolarization experiments. Au nanorods exhibit strongly anisotropic e-ph coupling dynamics. It is considered to arise from different weights of pump energy assigned to two polarization directions because of the anisotropy of Au nanorods rather than because of an intrinsic process. The e-ph coupling kinetics measured by transient experiments cannot be simply described by a single exponential function but by the integral of components contributed by random distribution of Au nanorods at all directions in aqueous solution. After this correction, the relationship between electron–phonon relaxation times and pump power is linear even in relatively high power. The time extrapolated to zero intensity is 0.75 ps, which is similar to the characteristic electron–phonon coupling time for nanodots and bulk Au.

Introduction

Considerable work has been done on metal nanoparticles recently because of their many interesting properties like enhanced near electromagnetic fields, wavelength tunable light absorption, and strong photothermal effect as well as potential technological applications including biological sensing, imaging, and nanoelectronic.^{1–22} Optical excitation of metal nanoparticles can lead to the collective oscillation of conduction-band electrons and can result in strong absorption of light. This absorption is called the surface plasmon resonance (SPR).^{22–26} The peak position and bandwidth of the plasmon band depend on several factors such as the size and shape of the nanoparticles, their dielectric constant, and the surrounding environment.^{22,24} One extensively studied system is the Au nanoparticle. For Au nanodots, the SPR absorption spectrum contains an intense absorption band in the visible region, while the SPR of Au nanorods splits into two modes: a longitudinal mode parallel to the long axis of the nanorod and a transverse mode perpendicular to it.^{27,28} The absorption peak of the transverse mode is essentially the same with SPR absorption of nanodots, while the longitudinal mode absorbs at lower energy and can be tuned by the aspect ratio.^{29,30}

In recent years, there has been a great deal of interest in investigating the electron dynamics in Au nanoparticles after excitation with femtosecond laser pulses.^{1–7,9–13,31–41} It is generally accepted that several photophysical processes contribute to the dynamics: electron–electron (e-e) scattering, electron–phonon (e-ph) coupling, and phonon–phonon (ph-ph) coupling. First, the excited electrons thermalize via e-e scattering on a time scale of tens to a few hundreds of femtoseconds resulting in the broadening of the plasmon absorption band and transient bleaches in the transient absorption

spectrum.^{10,11,13,33} Then, the hot electrons thermally equilibrate with the nanoparticle lattice through e-ph coupling with decay times of several picoseconds, which is followed by ph-ph coupling from heat dissipation to the environment with a slower decay on a few hundred picosecond time scale.^{1,31,33–35,37,38,40,41} Such a process is theoretically described by the so-called two-temperature model. The time constants of these relaxation processes are dependent on the excitation power and become longer as power increases.^{7,32,36,38,39} At low pump energy, the e-ph coupling times depend linearly on the pump energy. When pump energy is high, it shows a nonlinear behavior in Au nanorods.⁷

In general, the electron dynamics in Au nanorods is quite similar to that of nanodots even at a high aspect ratio of 25.⁴² However, nanorods obviously have strong anisotropic character, and the two modes have perpendicular polarization with each other. By aligning the nanorods in film or solid matrix,^{43,44} only one mode appears in a certain polarization direction. To the best of our knowledge, there is no report of transient depolarization experiments yet.

In this paper, femtosecond transient depolarization experiments were performed to investigate the anisotropic characteristics of e-ph coupling dynamics in Au nanorods. We find that the transient absorption spectra are strongly dependent on the probe polarization directions. However, the difference between the signals at two mutual perpendicular probe polarization directions is due to anisotropic pump energy rather than to anisotropy e-ph coupling of Au nanorods. The e-ph coupling transients in Au nanorods cannot be described as a single exponential function but as the integral of components contributed by randomly distributed Au nanorods in aqueous solution in the probe polarization direction. After this correction, the relationship between the e-ph coupling times and the pump energy is linear even in the relative high power range. The time extrapolated to zero intensity is in good agreement with the one

* To whom correspondence should be addressed. E-mail: haiyu_wang@jlu.edu.cn (H.-Y.W.); hbsun@jlu.edu.cn (H.-B.S.).

[†] College of Electronic Science and Engineering.

[‡] College of Physics.

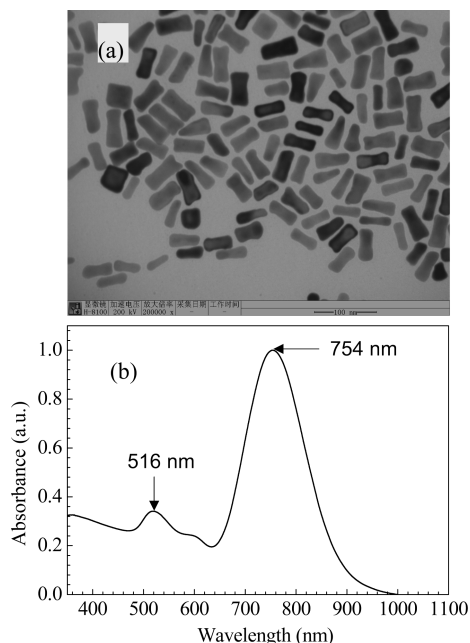


Figure 1. (a) Transmission electron micrograph of the Au nanorods. Their aspect ratio is 3.3 ± 0.5 with an average length of 50.0 ± 3.0 nm and a width of 14.7 ± 1.5 nm. (b) The normalized UV-vis-NIR absorbance spectrum of the aqueous nanorod solution. The transverse plasmon resonance peak is located at 516 nm while the longitudinal plasmon resonance peak is at 754 nm; the intermediate peak located at 610 nm is produced by a small percentage of nonrodlike nanoparticles.

measured at lower pump energy by other authors⁷ and is similar to the characteristic electron-phonon coupling time for bulk gold.⁴⁵

Experimental Section

Synthesis of Au Nanorods. A seed-mediated growth procedure slightly modified from that suggested by Jana et al. and Nikoobakht and El-Sayed^{46,47} was used to fabricate Au nanorods. First, a Au seed solution was prepared in a typical procedure. Cetyltrimethyl ammonium bromide (CTAB) solution (7.52 mL, 0.13 M) was mixed with 2.0 mL of 1 mM H₂AuCl₄. The solution appeared bright brown-yellow in color. To the stirred solution, 0.48 mL of ice-cold 0.01 M NaBH₄ was added all at once, which resulted in the formation of a pale brown-yellow solution. Vigorous stirring of the seed solution was continued for 2 min. After the solution was stirred, it was kept at 25 °C for future use. After 2 h, this seed solution was used for the synthesis of Au nanorods. In a flask, 77.25 mL of 0.2 M CTAB was mixed with 60 mL of 1 mM H₂AuCl₄ and 0.9 mL of 0.01 M silver nitrate aqueous solution after gentle mixing of the solution; 9.6 mL of 0.01 M L-Ascorbic acid (AA) was added with continuous stirring, and 2.25 mL of the seed solution was finally added into the mixture to initiate the growth of Au nanorods. A strong color change indicated the formation of the Au nanorods. These nanorods were aged for 5 h and were purified by several cycles of suspension in ultrapure water followed by centrifugation; nanorods were isolated in the precipitate, and excess CTAB was removed in the supernatant.

A transmission electron microscope (TEM, Hitachi H-8100 IV) was utilized to resolve the details of the nanorods operating at an acceleration voltage of 200 kV. The aspect ratio of the Au nanorod is around 3.3 ± 0.5 (length: 50.0 ± 3.0 nm, width: 14.7 ± 1.5 nm) (Figure 1a). At least 100 particles from each of the images were analyzed to yield the mean Au nanorod

dimensions. UV-vis-NIR spectra (Figure 1b) were measured with a Shimadzu UV-3101PC UV-vis-NIR scanning spectrophotometer in the 350–1100 nm range. The peaks of the transverse and longitudinal SPR are located at 516 and 754 nm, respectively.

Femtosecond Pump-Probe Experiments. The femtosecond transient absorption spectroscopy was performed as follows. The output of a Ti:Sapphire laser (Tsunami, Spectra Physics) pumped by an Nd:YVO laser (Millennia, Spectra Physics) was amplified in a regenerative amplifier (RGA, Spitfire, Spectra Physics). This generated laser pulses of 100 fs pulse width (half-width at half-maximum) and 0.4 mJ pulse energy centered at 800 nm with a repetition rate of 250 Hz. Twenty-five percent of the pulse energy was then used to generate a white light continuum as probe beam by focusing the beam into a 1 cm water cell. The remaining part was modulated by a synchronized optical chopper (Newport Model 75160) with a frequency of 125 Hz as the pump beam to excite the sample. Time-resolved transient absorption spectra were recorded with a highly sensitive spectrometer (Avantes AvaSpec-2048 × 14). The dynamics traces were obtained by controlling the relative delay between the pump and the probe pulses with a stepper-motor-driven optical delay line (Newport M-ILS250CC). The group velocity dispersion of the whole experimental system was compensated by a chirp program. The pump-probe measurements were carried out over a series of pump energy from 30 to 83 nJ per pulse, and the intensities of the pump pulses were measured with a laser power meter (Sanwa LP1). The sample of Au nanorods was circulated in a flow cell with a path length of 0.5 mm to ensure that a fresh sample volume was exposed to each pump pulse. The experimental data were fitted with a local written program running in Matlab on the basis of the proposed model. All the measurements were performed at room temperature.

Results and Discussion

Femtosecond transient depolarization experiments were performed in which the polarization of the probe beam was, respectively, parallel and perpendicular with respect to the polarized excitation beam. The pump energy varies from 30 to 83 nJ pulse⁻¹, which corresponds to power density from 2.2 to 6.1 GW/cm². UV-vis-NIR absorption spectra of the nanorods before and after laser experiments were measured to make sure that the sample used to record the transient absorption spectra was not photodamaged.

Transient Absorption Spectra. The pump pulse centered at 800 nm excites the SPR longitudinal mode of Au nanorods resulting in heating of the electrons within the conduction band.⁷ The increase in the electronic temperature changes the dielectric function of Au nanorods, which leads to the broadening of both plasmon absorption bands and to the decrease of the absorption intensity.¹³ These result in the bleaching of both the transverse and the longitudinal modes of the SPR and in the transient absorption signals in the wings of the two bands.

Transient absorption spectra at delay time of 0.4 ps obtained from two mutual perpendicular probe polarization directions at various pump energies are shown in Figure 2. The maximum of the transverse mode bleach band is located at 516 nm while the longitudinal mode bleach peak is located at 754 nm. Three additional positive absorption bands are observed at 484, 565, and 675 nm. The bleach maxima of the two plasmon bands in the transient absorption spectra coincide with the positions of the maxima in the steady-state spectrum. The positive absorption bands result from the broadened two SPR bands because of higher electronic temperatures. The spectrum with the wave-

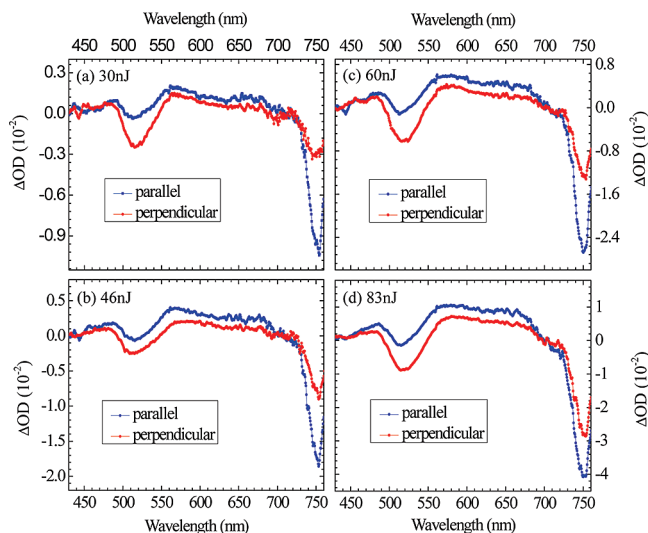


Figure 2. Transient absorption spectra measured from two mutual perpendicular probe polarization directions at 0.4 ps. Blue: polarization of the probe beam is parallel to the polarized excitation beam; red: polarization of the probe beam is perpendicular to the polarized excitation beam. The transverse bleach peak is located at 516 nm corresponding to the peak of transverse plasmon resonance peak, while the longitudinal bleach band is located at 754 nm which coincides with the longitudinal plasmon resonance peak. Pump energy: (a) 30, (b) 46, (c) 60, and (d) 83 nJ pulse⁻¹.

length greater than 760 nm is not shown because of the disturbance by the excitation.

Figure 2 shows that the transient spectra are strongly dependent on the probe polarization directions at all the pump energies. The bleach signal of the longitudinal mode has a larger magnitude when the polarization of the probe beam is parallel to that of the excitation beam. The bleach signals of the transverse mode at two probe directions show reversed trend. Clearly, this behavior is consistent with the anisotropic characters of Au nanorods in which the two modes have perpendicular polarization with each other.

Electron–Phonon Coupling Dynamics. The hot electrons thermally equilibrate with the nanoparticle lattice via e-ph coupling after the e-e scattering. This dynamical process can be monitored by the recovery of the SPR bleaching signals.^{1,31,32,36,39} Because the signals of the transverse mode detected at 516 nm is relatively weak, we will focus on the dynamics of the bleach peak located at 754 nm of the longitudinal mode for an example to better compare the difference of e-ph coupling dynamics between two mutual perpendicular probed directions.

Figure 3 shows the kinetics of the longitudinal bleach signals at 754 nm with various pump energies in which the polarization of the probe beam was parallel and perpendicular with respect to the polarized excitation beam. E-ph coupling and ph-ph coupling processes contribute to the dynamics. The fast decay component is due to the e-ph relaxation. The offset part corresponds to the ph-ph relaxation, which occurs on a time scale of 100 ps. The amplitude ratio of the ph-ph to the e-ph relaxation increases with increasing pump power. In the following discussion, we mainly focus on the e-ph coupling dynamics in Au nanorods.

As with previous reports, the e-ph relaxation time constants increase with the pump energy in both polarization directions (see Figure 3). At low pump power, previous experimental results have indicated that the e-ph relaxation times (range from 1.5 to 3 ps) are proportional to the pump power in Au nanodots and also in nanorods.^{7,32,36,38,39} Recently, it was found that at

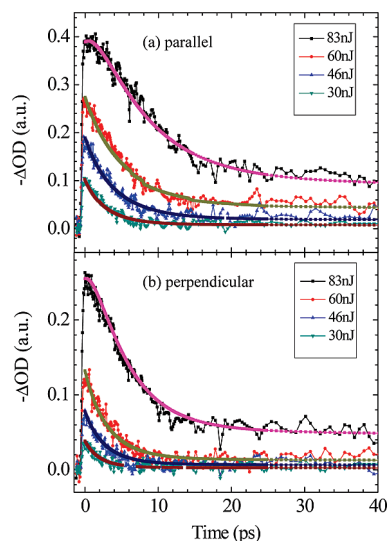


Figure 3. Bleach recovery kinetics monitored at 754 nm with various pump energy. From top to bottom, the pump energy is 83 nJ (square), 60 nJ (circle), 46 nJ (up triangle), and 30 nJ (down triangle) pulse⁻¹. The solid lines represent the fitting results with the proposed model. (a) Polarization of the probe beam is parallel to the polarized excitation beam; (b) polarization of the probe beam is perpendicular to the polarized excitation beam.

relatively high pump power, the relationship between the e-ph relaxation times of Au nanorods (range from 3 to 6 ps) significantly deviates from the linear behavior. By fitting the bleach recovery at 754 nm with single exponential decay, the e-ph relaxation times vary from 1.8 to 7 ps in our experiments, which cover both low and high pump power range.

Surprisingly, the fitting results show an unexpected anisotropic e-ph coupling dynamics for two probe directions, which differ not only in the magnitudes but also in the relaxation times. When probing at the perpendicular direction, the relaxation time is always short at the same pump power. As mentioned above, in current opinion, the electron dynamics can be described by a so-called two-temperature model. According to this model, the laser excitation creates a new electronic distribution at higher temperature, and this results in the SPR absorption having different amplitude and width, and so causes the transient signals. Clearly, this mechanism implies no difference between two modes, and so one would expect the observation of isotropic electron dynamics. Thus, this anisotropic e-ph coupling dynamics is unlikely an intrinsic phenomenon in Au nanorods. For the Au nanorod used here, according to the Stokes–Einstein relationship, the time constant of rotational diffusion is about 15 μ s, which is significantly longer than the time scale of electron–phonon relaxation. Thus, we can safely rule out this effect.

In fact, Au nanorod has strong anisotropic character: its longitudinal mode is parallel to the long axis of the nanorod. The effective light intensity to excite the longitudinal mode is the projection of pump intensity to the long axis of Au nanorod. If the polarization direction of probe light has been changed (equivalent to change excitation polarization), it will result in the different weights of pump energy assigned to two directions. This may be the reason for the unexpected anisotropic e-ph coupling dynamics. In the next section, we will further discuss these anisotropic e-ph coupling dynamics and also pump power dependent relaxation times by a simple theoretical model.

Theoretical Analysis. Suppose that a nanorod in aqueous solution locates in a direction relative to the probe polarization

direction with an angle of θ and is excited with the pump intensity of I_{pump} , and then the effective pump intensity of the polarization of the probe light parallel and perpendicular with respect to the polarized excitation light is $I_{\text{pump}} \times \cos^2 \theta$ and $I_{\text{pump}} \times 1/2 \sin^2 \theta$, respectively.⁴⁸ This implies that different weights of pump energy are assigned to two mutual perpendicular probing polarization directions originating from the anisotropy of the nanorod. If we assume that the e-ph coupling times are proportional to pump energy in the whole pump energy range we used, the relationship between them at two directions can be expressed as

$$\tau_{\text{e-ph}}^{\parallel} = \tau_{0(\text{e-ph})}^{\parallel} + b_{\parallel} I_{\text{pump}} \times \cos^2 \theta \quad (1a)$$

$$\tau_{\text{e-ph}}^{\perp} = \tau_{0(\text{e-ph})}^{\perp} + b_{\perp} I_{\text{pump}} \times \frac{1}{2} \sin^2 \theta \quad (1b)$$

where $\tau_{\text{e-ph}}^{\parallel}$ and $\tau_{\text{e-ph}}^{\perp}$ are the e-ph coupling times at two directions, $\tau_{0(\text{e-ph})}^{\parallel}$ and $\tau_{0(\text{e-ph})}^{\perp}$ are the intrinsic e-ph coupling times obtained by extrapolating the time to zero intensity for two polarization directions, and b_{\parallel} , b_{\perp} are the slopes.

We further assume that the amplitudes of the bleach signals are proportional to the pump energy. Then, the dynamics for a nanorod located with an angle of θ at two polarization directions can be described as

$$I_{\parallel}(t, \theta) \propto \cos^2 \theta [\exp(-t/(\tau_{0(\text{e-ph})}^{\parallel} + b_{\parallel} I_{\text{pump}} \times \cos^2 \theta))] \quad (2a)$$

$$I_{\perp}(t, \theta) \propto \frac{1}{2} \sin^2 \theta \left[\exp\left(-t/\left(\tau_{0(\text{e-ph})}^{\perp} + b_{\perp} I_{\text{pump}} \times \frac{1}{2} \sin^2 \theta\right)\right) \right] \quad (2b)$$

where $I_{\parallel}(t, \theta)$ and $I_{\perp}(t, \theta)$ are the amplitudes of transient bleach signals probed at two polarization directions as the function of time t and angle θ . Because of the random distribution and anisotropy of Au nanorods, the actual kinetics we detected is the integral of components contributed by randomly distributed Au nanorods in aqueous solution at all directions, which can be modeled as

$$I_{\parallel}(t) \propto \int_0^{\pi/2} \cos^2 \theta [\exp(-t/(\tau_{0(\text{e-ph})}^{\parallel} + b_{\parallel} I_{\text{pump}} \times \cos^2 \theta))] d\theta + c_{\parallel} \exp(-t/\tau_{\text{ph-ph}}^{\parallel}) \quad (3a)$$

$$I_{\perp}(t) \propto \int_0^{\pi/2} \frac{1}{2} \sin^2 \theta \left[\exp\left(-t/\left(\tau_{0(\text{e-ph})}^{\perp} + b_{\perp} I_{\text{pump}} \times \frac{1}{2} \sin^2 \theta\right)\right) \right] d\theta + c_{\perp} \exp(-t/\tau_{\text{ph-ph}}^{\perp}) \quad (3b)$$

The integrals show the e-ph coupling processes at two directions, while the second terms represent the ph-ph coupling processes, where $\tau_{\text{ph-ph}}^{\parallel}$ and $\tau_{\text{ph-ph}}^{\perp}$ are the ph-ph coupling times at two directions and c_{\parallel} and c_{\perp} are the relative amplitudes. In fact, the parameters for ph-ph coupling are taken from the results by directly fitting the offset part of the transients.

Figure 3 shows that the kinetics can be well fitted by the model using eq 3. There is a small rise component at very early times at pump energy of 83 nJ pulse⁻¹; it comes from a relatively slower e-e scattering process at higher pump power that is not

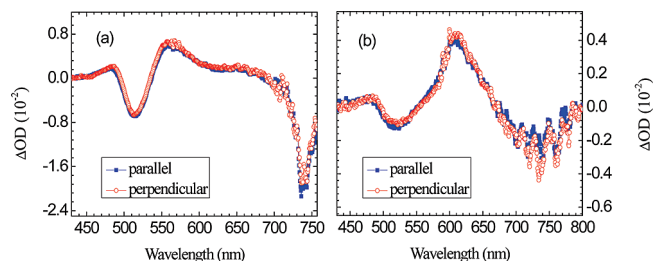


Figure 4. (a) Transient absorption spectra of circular polarization probe excited at 800 nm with mutual perpendicular polarization directions at 0.4 ps. (b) Transient absorption spectra measured from two mutual perpendicular probe polarization directions excited at 400 nm at 0.4 ps. Blue: polarization of the probe beam is parallel to the polarized excitation beam; red: polarization of the probe beam is perpendicular to the polarized excitation beam.

included in our model. Thus, we add an exponential rise term (1.5 ps, amplitudes about 30%) during fitting this kinetics.

The fitting results show that the values of b_{\parallel} and b_{\perp} are essentially the same at each pump energy, $b_{\parallel} = b_{\perp} = 0.11 \pm 0.01$ ps/nJ pulse⁻¹. This gives a strong support to our model. The observation dynamics are indeed the integral of components contributed by random distribution of Au nanorods in aqueous solution. The anisotropic e-ph coupling dynamics probed at two mutual perpendicular polarization directions is the result of different weights of pump energy ($I_{\text{pump}} \times \cos^2 \theta$ and $I_{\text{pump}} \times 1/2 \sin^2 \theta$) because of the anisotropy of Au nanorods.

The fitting also gives the same intrinsic e-ph coupling times $\tau_{0(\text{e-ph})} = 0.75$ ps for all the pump energies together with the same slopes b_{\parallel} and b_{\perp} , which indicate that the relationship between the e-ph coupling times and the pump energy in our experimental range is linear. The time extrapolated to zero intensity is 0.75 ps which is in good agreement with the one measured at lower pump energy ranging from 0.65 to 0.81 ps^{1,7,36} and which is similar to the characteristic electron–phonon coupling time for bulk Au.⁴⁵ Thus, the relationship of e-ph coupling times versus pump energy in our experimental range at each probe polarization direction coincides with rather than deviates from that measured at lower pump energy. We can give a more useful relationship of the electron–phonon relaxation times versus pump power density D_{pump} as

$$\tau_{\text{e-ph}}(\text{ps}) = 0.75 \text{ps} + 1.5 D_{\text{pump}} (\text{GW}/\text{cm}^2) \quad (4)$$

Finally, to further support this model, we have performed two additional experiments. First, if the anisotropic behavior is due to different weights of pump energy, it will disappear when the circular polarization probe is used. Figure 4a shows the transient absorption spectra of the circular polarization probe at delay time of 0.4 ps excited at 800 nm with two mutual perpendicular polarization directions. The results give a clearly isotropic spectra and also dynamics. Second, when the interband transitions are excited at 400 nm, they will also give an isotropic result since the interband excitation does not have polarization selection. As one can expect, the transient depolarization experiments excited at 400 nm also show perfect isotropic behavior; see Figure 4b. Our transient spectrum is consistent with that reported in ref 1 at the same 400 nm excitation. However, compared with the result at 800 nm excitation, the relative amplitude of the longitudinal mode bleach is much less and the spectrum is broad. This is because of nonselective excitation of the inhomogeneous nanorods with different aspect ratios.

Conclusion

Femtosecond transient depolarization experimental results show clearly anisotropic e-ph coupling dynamics in Au nanorods, which differs not only in the magnitudes but also in the relaxation times. However, this anisotropic e-ph coupling dynamics is not due to an intrinsic process but is the result of different weights of pump energy assigned to two directions because of the anisotropy of Au nanorods. The e-ph coupling kinetics measured by transient experiments cannot be simply described by a single exponential function but by the integral of components contributed by random distribution of Au nanorods at all directions in aqueous solution. After this correction, the relationship between electron–phonon relaxation times and pump power is linear even in relatively high power. The time extrapolated to zero intensity is 0.75 ps which is similar to the characteristic electron–phonon coupling time for nanodots and bulk Au.

Acknowledgment. The authors would like to acknowledge Natural Science Foundation, China (NSFC) under Grants No. 20973081, 60525412, and 60677016 and the 863 project of China Grant No. 2007AA03Z314 for support. We thank Ling-Yun Pan, Hong-Hua Fang, and Ya-Wei Hao for helpful discussions and also the reviewer's suggestions.

References and Notes

- (1) Link, S.; El-Sayed, M. A. *J. Phys. Chem. B* **1999**, *103*, 8410.
- (2) Link, S.; El-Sayed, M. A. *Annu. Rev. Phys. Chem.* **2003**, *54*, 331.
- (3) Hartland, G. V. *Annu. Rev. Phys. Chem.* **2006**, *57*, 403.
- (4) Varnavski, O. P.; Goodson, T., III; Mohamed, M. B.; El-Sayed, M. A. *Phys. Rev. B* **2005**, *72*, 235405.
- (5) Huang, W. Y.; Qian, W.; El-Sayed, M. A.; Ding, Y.; Wang, Z. L. *J. Phys. Chem. C* **2007**, *29*, 10753.
- (6) Ramakrishna, G.; Dai, Q.; Zou, J. H.; Huo, Q.; Goodson, T., III. *J. Am. Chem. Soc.* **2007**, *129*, 1848.
- (7) Park, S.; Pelton, M.; Liu, M.; Guyot-Sionnest, P.; Scherer, N. F. *J. Phys. Chem. C* **2007**, *111*, 116.
- (8) Pelton, M.; Liu, M.; Park, S.; Scherer, N. F.; Guyot-Sionnest, P. *Phys. Rev. B* **2006**, *73*, 155419.
- (9) Hartland, G. V. *Phys. Chem. Chem. Phys.* **2004**, *6*, 5263.
- (10) Voisin, C.; Christofilos, D.; Loukakos, P. A.; Del Fatti, N.; Vallée, F. *Phys. Rev. B* **2004**, *69*, 195416.
- (11) Voisin, C.; Del Fatti, N.; Christofilos, D.; Vallée, F. *J. Phys. Chem. B* **2001**, *105*, 2264.
- (12) Grant, C. D.; Schwartzberg, A. M.; Norman, T. J., Jr.; Zhang, J. Z. *J. Am. Chem. Soc.* **2003**, *125*, 549.
- (13) Link, S.; Burda, C.; Mohamed, M. B.; Nikoobakht, B.; El-Sayed, M. A. *Phys. Rev. B* **2000**, *61*, 6086.
- (14) Chen, S. W.; Pei, R. J. *J. Am. Chem. Soc.* **2001**, *123*, 10607.
- (15) Henglein, A. *J. Phys. Chem. B* **2000**, *104*, 6683.
- (16) Henglein, A.; Giersig, M. *J. Phys. Chem. B* **2000**, *104*, 5056.

- (17) Park, S.; Yang, P. X.; Corredor, P.; Weaver, M. J. *J. Am. Chem. Soc.* **2002**, *124*, 2428.
- (18) Park, J. I.; Cheon, J. *J. Am. Chem. Soc.* **2001**, *123*, 5743.
- (19) Krug, J. T.; Wang, G. D.; Emory, S. R.; Nie, S. M. *J. Am. Chem. Soc.* **1999**, *121*, 9208.
- (20) Averitt, R. D.; Westcott, S. L.; Halas, N. J. *Phys. Rev. B* **1998**, *58*, 10203.
- (21) Templeton, A. C.; Hostetler, M. J.; Warmoth, E. K.; Chen, S. W.; Hartshorn, C. M.; Krishnamurthy, V. M.; Forbes, M. D. E.; Murray, R. W. *J. Am. Chem. Soc.* **1998**, *120*, 4845.
- (22) Kreibig, U.; Vollmer, M. *Optical properties of metal clusters*; Springer: Berlin and New York, 1995.
- (23) Kerker, M. *The Scattering of Light and Other Electromagnetic Radiation*; Academic: New York, 1969.
- (24) Bohren, C. F.; Huffman, D. R. *Absorption and Scattering of Light by Small Particles*; John Wiley & Sons: New York, 1983.
- (25) Michaels, A. M.; Nirmal, M.; Brus, L. E. *J. Am. Chem. Soc.* **1999**, *121*, 9932.
- (26) Mie, G. *Ann. Phys. (Leipzig)* **1908**, *25*, 377.
- (27) Gans, R. *Ann. Phys. (Leipzig)* **1915**, *47*, 270.
- (28) Papavassiliou, G. C. *Prog. Solid State Chem.* **1980**, *12*, 185.
- (29) Mohamed, M. B.; Ismael, K. Z.; Link, S.; El-sayed, M. A. *J. Phys. Chem. B* **1998**, *102*, 9370.
- (30) Yu, Y.; Chang, S.; Lee, C.; Wang, C. R. C. *J. Phys. Chem. B* **1997**, *101*, 6661.
- (31) Ahmadi, T. S.; Logunov, S. L.; El-sayed, M. A. *J. Phys. Chem.* **1996**, *100*, 8053.
- (32) Ahmadi, T. S.; Logunov, S. L.; El-sayed, M. A.; Khoury, J. T.; Whetten, R. L. *J. Phys. Chem.* **1997**, *101*, 3713.
- (33) Perner, M.; Bost, P.; Plessen, G. V.; Feldmann, J.; Becker, U.; Mennig, M.; Schmidt, H. *Phys. Rev. Lett.* **1997**, *78*, 2192.
- (34) Zhang, J. Z. *Acc. Chem. Res.* **1997**, *30*, 423.
- (35) Inouye, H.; Tanaka, K.; Tanahashi, I.; Hirao, K. *Phys. Rev. B* **1998**, *57*, 11334.
- (36) Hodak, J. H.; Martini, I.; Hartland, G. V. *J. Phys. Chem. B* **1998**, *102*, 6958.
- (37) Roberti, T. W.; Smith, B. A.; Zhang, J. Z. *J. Chem. Phys.* **1995**, *102*, 3860.
- (38) Hodak, J. H.; Henglein, A.; Hartland, G. V. *J. Phys. Chem. B* **2000**, *104*, 9954.
- (39) Hodak, J. H.; Henglein, A.; Hartland, G. V. *J. Chem. Phys.* **2000**, *112*, 5942.
- (40) Hu, M.; Hartland, G. V. *J. Phys. Chem. B* **2002**, *106*, 7029.
- (41) Hu, M.; Hartland, G. V. *J. Phys. Chem. B* **2002**, *107*, 1284.
- (42) Sando, G. M.; Berry, A. D.; Owrutsky, J. C. *J. Chem. Phys.* **2007**, *127*, 074705.
- (43) van der Zande, B. M. I.; Pagès, L.; Hikmet, R. A. M.; van Blaaderen, A. *J. Phys. Chem. B* **1999**, *103*, 5761.
- (44) Atkinson, R.; Hendren, W. R.; Wurtz, G. A.; Dickson, W.; Zayats, A. V.; Evans, P.; Pollard, R. J. *Phys. Rev. B* **2006**, *73*, 235402.
- (45) Sun, C.-K.; Vallée, F.; Acioli, L. H.; Ippen, E. P.; Fujimoto, J. G. *Phys. Rev. B* **1994**, *50*, 15337.
- (46) Jana, N. R.; Gearheart, L.; Murphy, C. J. *Adv. Mater.* **2001**, *13* (18), 1389–1393.
- (47) Nikoobakht, B.; El-Sayed, M. A. *Chem. Mater.* **2003**, *15* (10), 1957–1962.
- (48) Lakowicz, J. R. *Principles of Fluorescence Spectroscopy*; 3rd ed.; Springer: Berlin/Heidelberg, 2006.

JP9108656